



Growth and structural characterization of well-aligned RuO₂ nanorods on LiNbO₃ (1 0 0) via MOCVD

P.C. Liao^a, C.A. Chen^b, J.G. Chi^b, Y.S. Huang^{b,*}, D.S. Tsai^c, K.K. Tiong^d

^a Department of Electronic Engineering, Technology and Science Institute of Northern Taiwan, Taipei 112, Taiwan

^b Department of Electronic Engineering, National Taiwan University of Science and Technology, Taipei 106, Taiwan

^c Department of Chemical Engineering, National Taiwan University of Science and Technology, Taipei 106, Taiwan

^d Department of Electrical Engineering, National Taiwan Ocean University, Keelung 202, Taiwan

ARTICLE INFO

Article history:

Received 26 June 2008

Received in revised form

15 September 2008

Accepted 17 September 2008

Available online 25 November 2008

PACS:

81.07.Bc

81.15.Gh

61.05.C-

61.46.-w

Keywords:

Oxide materials

Nanorods

Metal-organic chemical vapor deposition

Scanning electron microscopy

X-ray diffraction

ABSTRACT

We report the preparation of well-aligned RuO₂ nanorods (NRs) on LiNbO₃(1 0 0) by metal-organic chemical vapor deposition using bis(ethylcyclopentadienyl) ruthenium (II) as the source reagent. The surface morphology and structural properties of the as-grown NRs were characterized by using field emission scanning electron microscopy and X-ray diffractometry. The growth pattern initiated with nucleation of both (0 0 1) and (3 0 1) planes at the substrate surface, but eventually NRs with (0 0 1) growth plane outgrew and formed vertically aligned NRs on top of the mixed alignments at the interface. The observed epitaxial growth patterns are explained in terms of the relationship between the atomic arrangements of the substrate and the NRs and the *c*-directional growth mechanism.

© 2008 Elsevier B.V. All rights reserved.

1. Introduction

Recently, a wide range of the nanosized oxide materials become the focus of intensive research owing to their fundamental interests in science and potential in fabrication nanodevices [1,2]. Among the numerous oxides, the electrically conducting RuO₂ belongs to the family of transition-metal dioxide compounds with a rutile structure [3] which exhibits high thermal and chemical stability. RuO₂ has been used as an electrode material for electrochemical devices [4], electrochemical capacitors for energy storage [5,6] and as field emission (FE) cathodes for vacuum microelectronic devices and displays [7,8]. As a result of these diverse applications, there is a growing need to develop easy and reliable methods for synthesizing RuO₂ phases as thin films or in other physical forms. Among the various growth techniques, metal-organic chemical vapor deposition (MOCVD) has demonstrated many advantages over others

including better composition control, higher deposition rate, excellent step coverage and suitability for scale-up [9]. Hence, it is worth exploring for the growth of RuO₂ nanocrystals (NCs) by MOCVD.

In this report, we present the results of deposition RuO₂ nanorods (NRs) on LiNbO₃ (LNO) (1 0 0) via MOCVD. The morphology and structural properties of the as-deposited NRs were characterized using field emission scanning electron microscopy (FESEM) and X-ray diffractometry (XRD). Two distinct growth planes, (0 0 1) and (3 0 1), were found to be energetically favorable for epitaxial growth of RuO₂ NRs on LNO(1 0 0). The possible mechanisms for the growth of well-aligned NRs are discussed.

2. Experimental

RuO₂ NRs depositions were carried out in a cold-wall reactor, using bis(ethylcyclopentadienyl) ruthenium (II) as the source reagent on the LNO(1 0 0) substrates (~10 mm × 10 mm). Two independent thermal couples were mounted on the source transport line to control and monitor the temperature of the gas transfer line (*T*_{tl}) and the precursor reservoir (*T*_{pr}). During the source vapor transport *T*_{tl} and *T*_{pr}, controlled by two independent controllers, were kept at 150 and 180 °C, respectively, to avoid precursor condensation during the vapor-phase transport. An oxygen flow rate of 20 sccm was used to transport precursor vapor and to invoke the

* Corresponding author. Tel.: +886 2 27376385; fax: +886 2 27376424.
E-mail address: ysh@mail.ntust.edu.tw (Y.S. Huang).

growth reaction. An oxygen pressure of ~ 5 mbar was applied, while deposition temperature was fixed at 500°C . A JEOL-JSM6500F FESEM with an accelerating voltage of 15 kV was used to study the morphology of RuO_2 NRs. The growth orientations were examined using a Rigaku D/Max-RC X-ray diffractometer equipped with $\text{Cu K}\alpha$ ($\lambda = 1.5418 \text{ \AA}$) radiation source and Ni filter.

3. Results and discussion

FESEM micrographs depicted in Fig. 1(a)–(c) display images of RuO_2 NRs deposited on LNO(1 0 0) with various deposition times. As can be seen in Fig. 1(a), at the very beginning a thin RuO_2 film forms on the substrate surface and serves as the root layer for growing RuO_2 NRs. As shown in Fig. 1(b), both vertically aligned and tilted (with similar tilted angle ($\sim 64^\circ$) from the normals to the substrate) RuO_2 NRs were grown on the same substrate. It was determined from the XRD patterns that the vertically aligned and the tilted NRs were those of (0 0 1) and (3 0 1) planes, respectively. Those grains with the (0 0 1) plane facing the gas phase will grow upwards faster than other grains and turn into vertically aligned nanorods as depicted in Fig. 1(c).

Fig. 2(a) shows the X-ray θ – 2θ scan data of a typical RuO_2 NRs grown on LNO(1 0 0). In addition to the LNO 3 0 0 substrate signal, the spectrum show two features at $\sim 59.5^\circ$ and $\sim 69.5^\circ$ corresponding to RuO_2 0 0 2 and 3 0 1 diffraction peaks, respectively. The insets in Fig. 2(a) show the rocking curves (θ scan) of 0 0 2 and 3 0 1. The

full width at half maximum (FWHM) for 0 0 2 and 3 0 1 peaks are 3.28° and 2.10° , respectively, indicating a relatively good alignment of the NRs. Fig. 2(b) shows the increase of the relative intensity ratio I_{002}/I_{301} of RuO_2 NRs on deposition time. As the deposition time is increased, the content of vertically aligned NRs exceeded those of the tilted NRs.

To determine the directions of planar deposition the atomic arrangements of appropriate surfaces need to be examined. Fig. 3 illustrates the schematic plots of the atoms arrangements and lattice relationships between RuO_2 and LNO(1 0 0) surfaces. The lattice parameters are $a = b = 4.49 \text{ \AA}$ and $c = 3.11 \text{ \AA}$ for RuO_2 [JCPDS No. 88-0322], $a = b = 5.15 \text{ \AA}$ and $c = 13.86 \text{ \AA}$ for LiNbO_3 [JCPDS No. 20-631]. As shown in Fig. 3 the oxygen anion patterns of both the (0 0 1) and (3 0 1) planes are very similar to that of LNO(1 0 0), where (0 0 1) plane shows a higher degree of lattice mismatch. During the initial stage of NRs formation onto the substrate surface, the oxygen atoms from the RuO_2 have sufficient surface mobility to align themselves with the existing oxygen sublattice of the LNO(1 0 0) in order to form an initial structural network of oxygen atoms. The alignment of $\text{RuO}_2(0 0 1)$ on LNO(1 0 0) produces directional mismatches on LNO(1 0 0) of -12.8% and -3.2% along LNO[0 1 0] and LNO[0 0 1], respectively. For $\text{RuO}_2(3 0 1)$ on LNO(1 0 0), the directional mismatches are $+1\%$ and -3.2% along LNO[0 1 0] and LNO[0 0 1], respectively. This argument of minimization of oxide sublattice structural mismatch prescribed two possible NRs-substrate

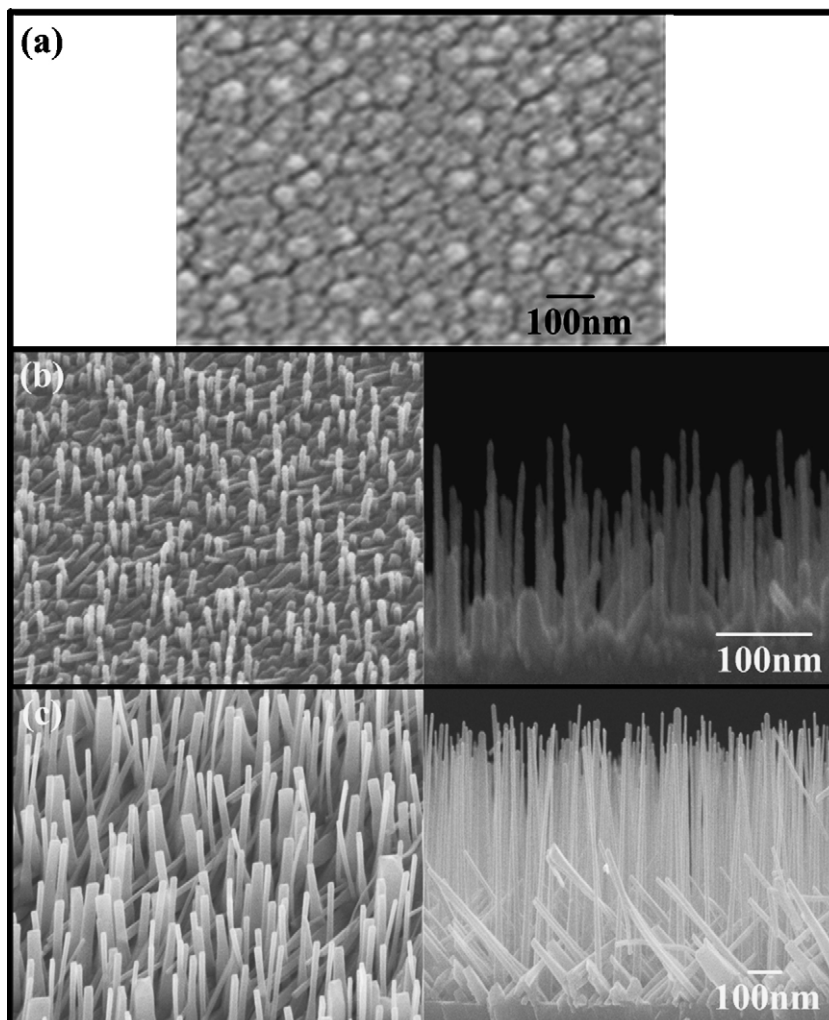


Fig. 1. FESEM images of RuO_2 NRs deposited on LNO(1 0 0) with various deposition times (a) $t = 30$ s, (b) $t = 15$ min and (c) $t = 60$ min.

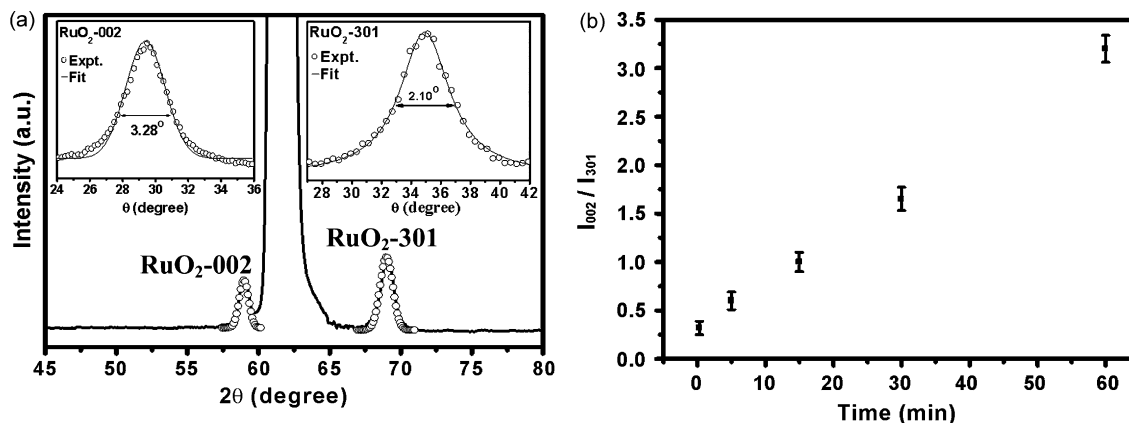


Fig. 2. (a) The X-ray θ - 2θ scan data of a typical RuO₂ NRs grown on LNO(100). The insets are the rocking curves (θ scan) of RuO₂ 002 and 301 diffraction peaks. (b) The relative intensity ratio I_{002}/I_{301} of RuO₂ NRs vs. deposition time.

alignments of RuO₂(001)[100][010]//LNO(100)[010][001] and RuO₂(301)[10 $\bar{3}$][010]//LNO(100)[010][001]. Accordingly, the resultant oxygen arrangement in the layer can form two groups of dominate grains with (001) and (301) planes.

The growth kinetics of well-aligned NRs is further guided by the important internal factor of c -directional growth mechanism [10,11]. The other parameters such as growth conditions

and substrate orientations are classified as the external factors. The c -directional growth mechanism comes from the anisotropy of the crystal structure that results in different growth rate for the different directions of NCs. The external factors such as the substrate orientation combined with temperature of substrate can influence the internal factors such as energetically favorable surface for the incoming atoms and initiate the preferable plane

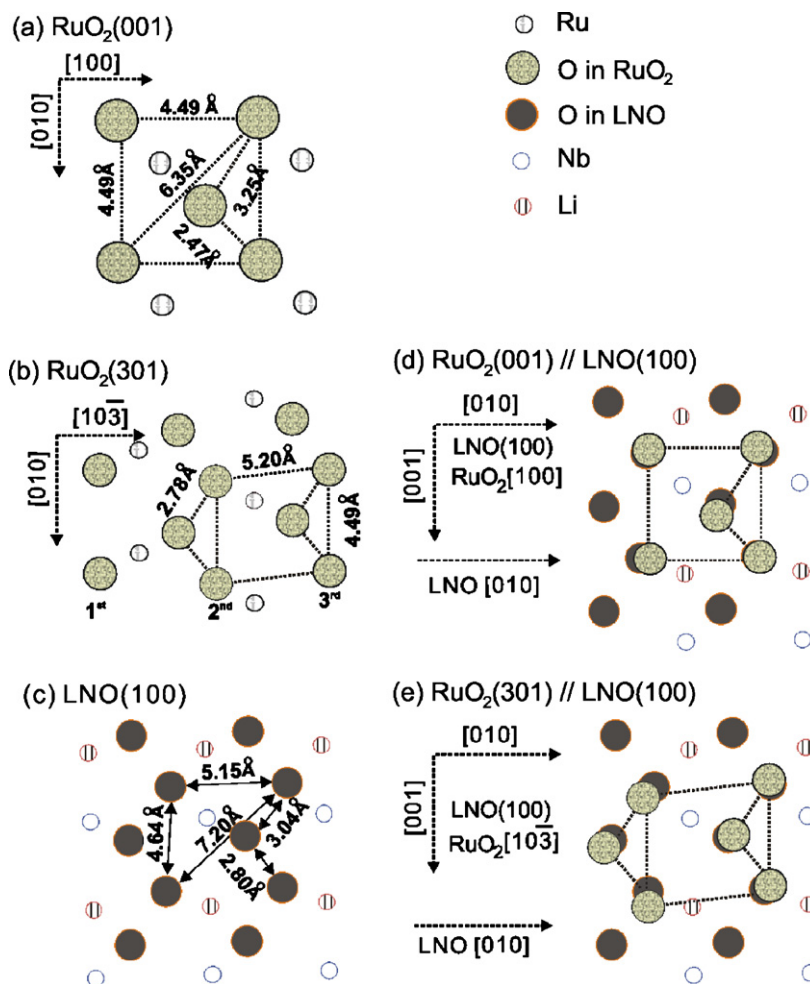


Fig. 3. The schematic plots of the atoms arrangements and lattice relationships between RuO₂ and LNO(100) surfaces: (a) RuO₂(001) plane; (b) RuO₂(301) plane; (c) LNO(100) plane; (d) RuO₂(001) on LNO(100); (e) RuO₂(301) on LNO(100).

orientation of RuO₂ NRs, whereby the incoming atoms will stick on the lower energy sites. The minimization of the oxide sublattice structural mismatch overlapping with the *c*-directional growth mechanism would then form the main driving force for the formation of well-aligned RuO₂ 1D NRs. The grains with (001) plane facing the gas phase tends to receive more incoming atoms and will grow upwards faster than grains with (301) plane resulting in predominantly vertically aligned (001) NRs as time progresses.

4. Summary

Morphology and growth planes of RuO₂ NRs on LNO(100) substrates have been systematically studied as a function of deposition time. The growth pattern initiated with nucleation of both (001) and (301) planes at the substrate surface, but eventually NRs with (001) growth plane outgrew and formed a vertically aligned NRs on top of the mixed alignments at the interface. The strong substrate effect on the RuO₂ NRs' alignment can be interpreted as the combined effects of the minimization of the oxide sublattice structural mismatch and the *c*-directional growth mechanism. As-deposition time progresses, the eventual alignment of the NRs will then be dominated by the growth plane with the lowest

sticking energy, i.e. the most energetically favorable (001) growth plane.

Acknowledgement

The authors acknowledge the support of the National Science Council of Taiwan under Contract No. NSC 96-2112-M-011-001.

References

- [1] Y. Xia, P. Yang, Y. Sun, Y. Wu, B. Mayers, B. Gates, Y. Yin, F. Kim, H. Yan, *Adv. Mater.* 15 (2003) 353–389.
- [2] G.R. Patzke, F. Krumeich, R. Nesper, *Angew. Chem. Int. Ed. Engl.* 41 (2002) 2446–2461.
- [3] R.S. Chen, Y.S. Huang, Y.L. Chen, Y. Chi, *Thin Solid Films* 413 (2002) 85–91.
- [4] S. Ferro, A.J. de Battisti, *J. Phys. Chem. B* 106 (2002) 2249–2254.
- [5] Y.F. Ke, D.S. Tsai, Y.S. Huang, *J. Mater. Chem.* 15 (2005) 2122–2127.
- [6] D. Susanti, D.S. Tsai, Y.S. Huang, A. Korotcov, W.H. Chung, *J. Phys. Chem. C* 111 (2007) 9530–9537.
- [7] C.S. Hsieh, G. Wang, D.S. Tsai, R.S. Chen, Y.S. Huang, *Nanotechnology* 16 (2005) 1885–1891.
- [8] A. Korotcov, Y.S. Huang, T.Y. Tsai, D.S. Tsai, K.K. Tiong, *Nanotechnology* 17 (2006) 3149–3153.
- [9] F. Maury, *Chem. Vapor Deposition* 2 (1996) 113–115.
- [10] A. Korotcov, H.P. Hsu, Y.S. Huang, D.S. Tsai, K.K. Tiong, *Cryst. Growth Des.* 6 (2006) 2501–2506.
- [11] R.S. Chen, A. Korotcov, Y.S. Huang, D.S. Tsai, *Nanotechnology* 17 (2006) R67–R87.